ELSEVIER

Journal of Nuclear Materials 266–269 (1999) 1078–1083

journal of nuclear materials

Carbon impurity behavior in w-shaped pumped divertor of JT-60U

S. Higashijima [a,*], H. Kubo [a], T. Sugie [a], K. Shimizu [a], A. Kumagai [b], A. Sakasai [a], N. Asakura [a], S. Sakurai [a], N. Hosogane [a], S. Konoshima [a], H. Tamai [a], T. Ishijima [b], H. Takenaga [a], K. Itami [a], M. Shimada [a]

[a] *Japan Atomic Energy Research Institute, Naka Fusion Research Establishment, 801-1 Mukouyama, Naka-machi, Naka-gun, Ibaraki-ken 311-0193, Japan*

[b] *Plasma Research Center, University of Tsukuba, Ibaraki-ken 305, Japan*

Abstract

The divertor geometry of JT-60U was modified from an open type to a w-shaped pumped configuration. This paper discusses behavior of carbon impurity in the w-shaped divertor. Carbon generation by chemical sputtering is important in deuterium plasmas. The reduction of carbon generation in helium discharges is consistent with this conclusion. CD-band intensities in the private flux region were smaller in the w-shaped divertor than in the open divertor, suggesting that the divertor dome is effective in decreasing chemically sputtered hydrocarbon molecules. The observed CD-band intensity was fairly reproduced by simulation using the IMPMC-code. When deuterium gas was puffed into the divertor, Z_{eff} value in the main plasma became about 15% larger than with puffing from the main chamber. For reducing impurity in the main plasma, the gas puffing from the top of main plasma was effective. © 1999 Elsevier Science B.V. All rights reserved.

Keywords: JT-60U; Divertor; Carbon; Chemical sputtering; Impurity transport

1. Introduction

To realize a tokamak reactor, it is necessary to simultaneously realize high performance in the main plasma and cold and dense divertor plasma. For this purpose, divertor was modified in the various machines and divertor physics has been investigated [1–3]. In JT-60U, divertor geometry was modified from an open divertor to a w-shaped pumped divertor to demonstrate cold and dense divertor [4].

When a cold and dense divertor plasma is formed, carbon generation by physical sputtering is suppressed and the chemical sputtering is the dominant carbon generation mechanism. Therefore, reduction of carbon impurities generated by chemical sputtering is important. In previous studies of impurity generation mechanism in JT-60U, it was concluded that carbon generation mechanism near the strike points could be explained by deuterium, oxygen and carbon sputtering (physical sputtering) in high power (~22 MW) NB heating discharges. The contribution of chemical sputtering by deuterium was small but chemical sputtering by oxygen was important [5,6]. However, an analysis with a two-dimensional impurity code based on Monte Carlo techniques (IMPMC-code) showed that the profiles of C II intensity in the private flux region could be explained with hydrocarbon molecule formation (e.g. methane CD_4) by chemical sputtering in high density discharges [7]. Dependence of chemical sputtering on deuterium ion flux and surface temperature was investigated, and the chemical sputtering yield was experimentally estimated [8]. These analyses also showed that methane generated in the private flux region by chemical sputtering easily reached the

* Corresponding author. Tel.: +81 29 270 7349; fax: +81 29 270 7419; e-mail: higashij@naka.jaeri.go.jp.

0022-3115/99/$ – see front matter © 1999 Elsevier Science B.V. All rights reserved.
PII: S0022-3115(98)00562-5

x-point SOL region. These analyses motivated us to implement the divertor dome.

There are two questions on impurity to be addressed in the divertor experiments after the modification. The first is whether hydrocarbon molecules that reach near the x-point can be reduced by the divertor dome or not (dome effect). The second is whether carbon impurity in the main plasma is reduced, and its transport in the divertor region is changed by the combination of gas puffing and pumping (puff and pump effect).

In this paper, we discuss the difference of carbon impurity generation between helium and deuterium plasmas and it is demonstrated that carbon generation by chemical sputtering is important in Section 3. In Section 4, the dome effect is investigated by comparing carbon impurity before and after the modification. Finally in Section 5, the puff and pump effects on carbon impurity are presented.

2. W-shaped pumped divertor

Fig. 1 shows the divertor geometry, the diagnostics and plasma configuration in the divertor region before [Fig. 1(a)] and after the divertor modification [Fig. 1(b)]. The w-shaped divertor consists of inner and outer baffle plates, divertor target tiles, a divertor dome and an aperture for pumping. The plasma facing components are covered with carbon tiles except for RF launchers. The baffle plates minimize leakage of neutral particles from the divertor chamber with a high neutral pressure to the main chamber. The divertor targets are inclined to expand the area of high heat flux. The dome in the private flux region separates the inner and outer divertor to improve the pumping efficiency from the inner private region where neutral density becomes higher. The second action of divertor dome is that it reduces the private volume and prevents chemically sputtered hydrocarbon molecules, e.g., methane, from easily reaching the x-point and penetrating the main plasma across the separatrix.

During the divertor modification, new density control tools, such as divertor pump and gas puff system, were installed. Three puffing inlets were installed at the top of main plasma (main puff) and two divertor puffing inlets were installed under the inner baffle plate (divertor puff). Particles are exhausted through the toroidally continuous pumping aperture in the inner leg side in the private flux region. And then, particles are conducted under the divertor dome and outer baffles and led to three cryo-pumps [9]. The main gas puffing fuels mainly the main plasma, whereas some particles from the divertor gas puffing are exhausted directly and contributed modestly to the main plasma fueling. Therefore, the puffing rate needed to keep the same main plasma density is larger with the divertor gas puff than with the main gas puff.

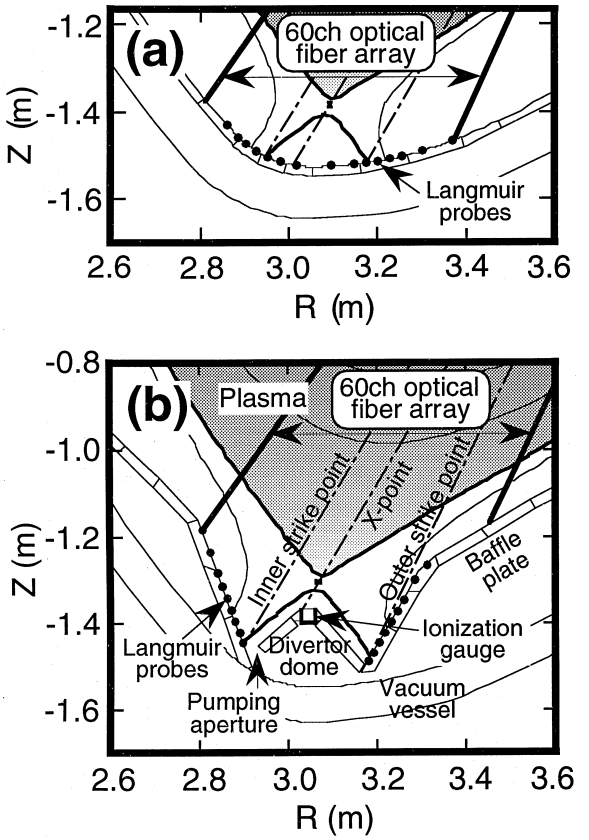

Fig. 1. Divertor geometry, the diagnostics and plasma configuration in the divertor region (a) before and (b) after the divertor modification.

The spatial emission profiles of deuterium and carbon impurity are measured with an absolutely calibrated 60-channel optical fiber array. This fiber array divides the light through a 60-channel optical fiber array into four parts (4×60 ch) and spatial profiles of four wavelengths are measured along the same sight lines simultaneously by interference filters. In the present experiment, CD-band (wavelength: ~430.5 nm), C II (657.8 nm), C IV (580.1 nm) and D_α (656.1 nm) intensities were measured. Then the spectra inside and outside the divertor dome in the wavelength from 411 to 453 nm around CD-band and D_γ were measured with a visible spectrometer.

In the divertor, 15 Langmuir probes were installed before the modification and 18 Langmuir probes have been installed during the modification. The estimated profiles of electron density and temperature were used for the simulation analysis of IMPMC-code. During the modification a fast response ionization gauge has been installed on the top of the divertor dome [10].

3. Carbon impurity generation in deuterium and helium plasmas

In helium and deuterium plasmas, hydrocarbon formation was investigated. This experiment was executed in high density OH plasmas. The discharge condition was as follows: $I_p = 1.2$ MA, $B_t = 3.5$ T, $q_{eff} \sim 6.5$, plasma volume ~ 57 m^3, height of x-point from the top of the divertor dome ~ 0.07 m. The electron density was gradually increased up to the density limit. As this experiment was carried out in the wall conditioning period just after boronization, in deuterium plasma there was a small amount of oxygen ($n_O/n_e \sim 0.1\%$) but a large amount of boron impurity ($n_B/n_e \sim 2\%$) existed and the density limit was a line averaged n_e(main) $\sim 1.8 \times 10^{19}$ m^{-3}. On the contrary, the density limit in helium discharges was the line averaged n_e(main) $\sim 5.0 \times 10^{19}$ m^{-3}. Thus, the density limit was much higher in helium plasmas than in deuterium plasmas.

Fig. 2(a) shows typical spectra in the outboard region from the divertor dome in deuterium and helium plasmas. The line averaged densities in the main plasma were 1.6×10^{19} m^{-3}. In helium plasmas, CD-band and D_γ spectra were not observed and the C II spectrum due to physical sputtering was small. On the other hand, in deuterium plasmas, D_γ, C II and CD-band spectra were obviously observed. He I spectrum was also found in deuterium plasmas because the deuterium discharges were made after helium discharges, and there was some helium remnant in the vacuum vessel. Fig. 2(b) shows the density dependence of intensities of CD-band and C II line in helium and deuterium plasmas. The change of electron temperature at the outer strike point was as follows: in helium plasmas T_e decreased monotonously from $\sim$40 eV (line averaged n_e(main) $= 1.0 \times 10^{19}$ m^{-3}) to $\sim$10 eV (line averaged n_e(main) $= 3.8 \times 10^{19}$ m^{-3}) and in deuterium plasmas T_e decreased monotonously from $\sim$40 eV (line averaged n_e(main) $= 1.0 \times 10^{19}$ m^{-3}) to $\sim$15 eV (line averaged n_e(main) $= 1.8 \times 10^{19}$ m^{-3}). In helium plasmas, the CD-band intensity was zero and the C II intensity was small and constant. In the high density regime with line averaged n_e(main) higher than 3.0×10^{19} m^{-3}, C II intensities decreased because electron temperature became 10–15 eV and physical sputtering yield of carbon by helium ions was small. On the contrary, in deuterium plasmas, CD-band and C II intensities increased with increasing electron density. In both plasmas the electron temperature near the outer strike point was $\sim$40 eV in the low density region around 1.0×10^{19} m^{-3}. With $T_e \sim 40$ eV, the incident energy of ion is estimated to be $\sim$120 eV and the physical sputtering yield of carbon by helium ion is about three times higher than the yield by deuterium ion [11]. The amount of sputtered carbon has not been estimated correctly yet, but the number of physically sputtered carbon ion in helium plasmas must be more than in deuterium plasmas. This led us to conclude that chemical sputtering contributes more in carbon generation than physical sputtering in deuterium plasmas.

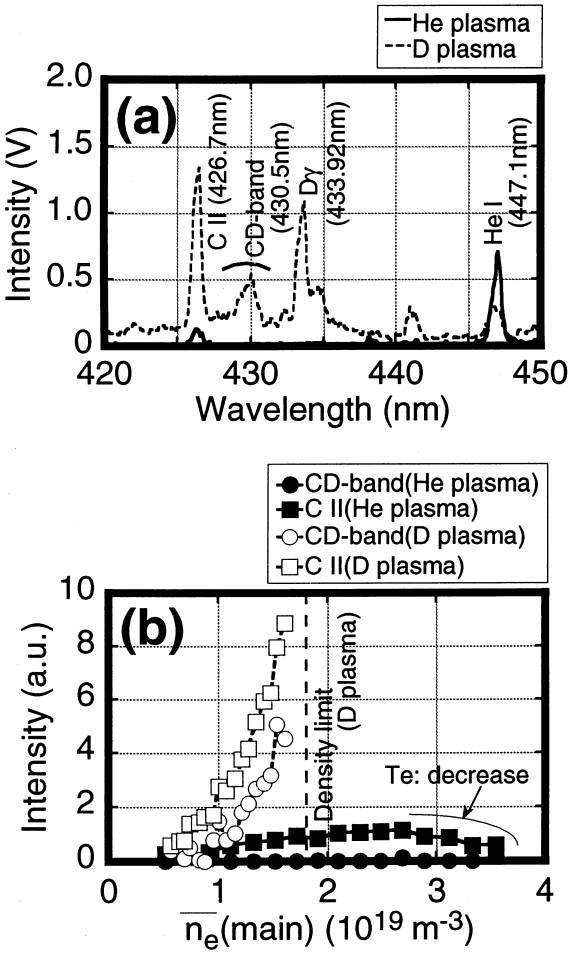

Fig. 2. (a) Typical spectra in the outboard region from the divertor dome in He and D plasmas when the line averaged density was 1.6×10^{19} m^{-3} and (b) density dependence of CD-band and C II spectra in He and D plasmas.

4. The effect of the divertor dome on carbon impurity production

One of the actions of the divertor dome is to prevent hydrocarbon molecules from reaching the x-point and to decrease carbon impurity in the main plasma. In this section, we discuss the effects of the divertor dome on carbon impurity.

This experiment was carried out in L-mode plasmas (NB power $\sim$4 MW). The line averaged density was gradually increased up to the density of MARFE onset. The discharge condition was as follows: $I_p = 1.2$ MA,

$B_t = 3.5$ T, plasma volume before the modification ~70 m^3 and ~57 m^3 after the modification, height of x-point before the modification ~0.14 m and the height of x-point ~0.07 m from the top of divertor dome after the modification, and the working gas was deuterium. After the modification the effects of divertor dome were investigated with a gas puff from the top of main plasma and without pumping.

Fig. 3 shows CD-band intensity profiles (a) before and (b) after the modification. The dotted and solid lines correspond to the low density case [line averaged electron density = 1.3×10^{19} m^{-3}] and the high density case [line averaged electron density = 1.8×10^{19} m^{-3}], respectively. CD-band intensities in the private flux region increased with the electron density. The increase rate was reduced by about 40% after the modification. This suggests the effect of the divertor dome on hydrocarbon molecules.

As the sight lines were different before and after the modification, it is difficult to compare intensities in these figures directly. Here, averaged intensities between the inner and the outer strike points, namely in the whole private flux region (shadow region in Fig. 3), are described. The averaged intensities of D_α line in the private flux region was larger after the modification than before the modification. The ratio of D_α line intensities after and before the modification, $r(D_\alpha) = D_\alpha^{after}/D_\alpha^{before}$, was 2 at the low electron density [line averaged $n_e(\text{main}) = 1.3 \times 10^{19}$ m^{-3}] and about 1.4 at high electron density [line averaged $n_e(\text{main}) = 1.8 \times 10^{19}$ m^{-3}]. The ratio of CD-band intensities after and before the modification, $r(CD) = CD^{after}/CD^{before}$, was 1.1 (low density) and about 0.75 (high density). The $r(CD)$ decreased with increasing electron density. This suggests that hydrocarbon molecules were decreased because of decrease of $r(D_\alpha)$. In other words, divertor dome suppresses the increment of neutral density in private flux region with increasing electron density. Chemical sputtering yield of carbon tiles should not change before and after the modification but $r(CD)/r(D_\alpha)$ was not unity. This suggests that the divertor dome is effective in reducing chemically sputtered hydrocarbon molecules that reach near the x-point; the transport of hydrocarbon molecules was modified before and after the modification. However, C II intensity increased after the modification in the divertor region and the Z_{eff} value in the main plasma was almost the same (2.5–2.6) before and after the modification. Carbon impurity generation is therefore not yet completely understood.

A two-dimensional impurity code based on Monte Carlo technique (IMPMC-code) was developed to study the impurity behavior in the divertor plasma [7]. The dissociation processes of methane sputtered by deuterium neutrals were simulated. The electron excitation rate coefficient for CD-band in Ref. [12] was used in the calculation. Fig. 4 shows the measured and calculated profiles of CD-band intensity after the modification. The calculated intensity of CD-band agrees well with the measurement within a factor of ~2.5. Understanding the distribution of measured C II and C IV is future work.

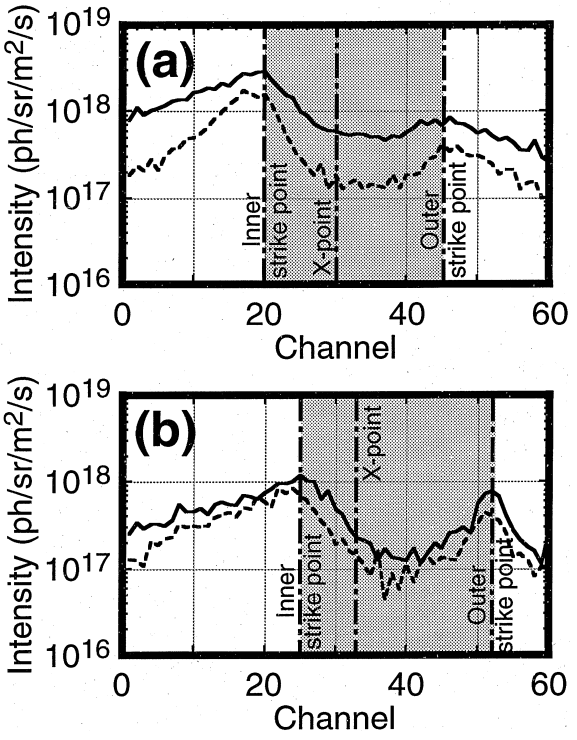

Fig. 3. CD band intensity profiles (a) before and (b) after the divertor modification. Dotted lines and solid lines correspond to the line averaged $n_e(\text{main}) = 1.3 \times 10^{19}$ m^{-3} and the line averaged $n_e(\text{main}) = 1.8 \times 10^{19}$ m^{-3}, respectively. The shadow zone is the private flux region.

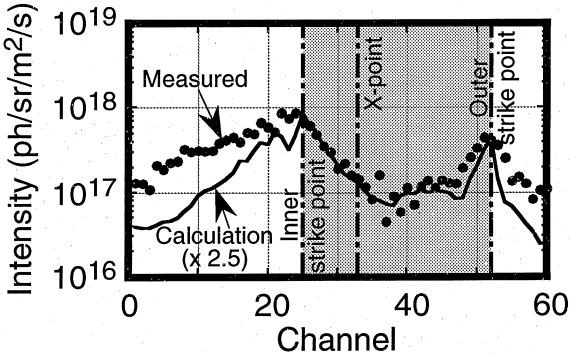

Fig. 4. CD-band intensity profiles. Dots: measurement. Solid line: IMPMC-code calculation multiplied by 2.5.

5. The effect of the gas puffing and pumping on carbon impurities

New density control tools, such as a divertor pump and gas puff system, were installed during the divertor modification. It is expected that SOL flow is produced by the combination of gas puffing and pumping. Therefore, the effects of puff and pump on carbon impurity in the main plasma and in the divertor region were investigated.

This experiment was carried out in L-mode plasmas (NB power ~4 MW). The electron density was gradually increased up to the MARFE onset density by the feedback control. The discharge condition was as follows; $I_p = 1.2$ MA, $B_t = 3.5$ T, height of x-point from the top of the divertor dome ~0.07 m and the working gas was deuterium.

Z_{eff} values in the main plasma and MARFE onset densities with pumping are shown in Fig. 5. The Z_{eff} values with the main puff were lower by about 15%, compared to those with the divertor puff, but they were not different with and without pumping. The MARFE onset densities were higher with the main puff by ~10% than with the divertor puff, and the onset densities were almost the same with and without pumping. With line averaged n_e(main) of 1.75×10^{19} m^{-3}, the puffing rates with pumping were 12 Pa m^3/s with the main puff and 15 Pa m^3/s with the divertor puff. The particles fueled with the main gas puff corresponded to ~7% of recycling particles in the divertor.

There are two reasons for decrease of Z_{eff} values in the main plasma. The first is that the effect of puff and pump generates the SOL flow, pushing back the impurity ions by the friction force. For example, in H-mode plasmas the decay time of neon ions in the main plasma became shorter with the puffing rate of main gas puff [13]. The second is that impurity generation in the divertor changes with different positions of gas puff. Fig. 6 shows D_α line and CD-band intensity profiles in the divertor region. The CD-band intensity was almost the same in the inboard region of inner strike point and the outboard one of outer strike point. But the CD-band intensity in the private flux region was different, and the intensity was smaller with the main puff than with the divertor puff. Profiles of C II and C IV intensities also showed the same tendency. D_α line intensities in the private flux region with the divertor puff were two times larger than with the main puff. Neutral pressure measured with a fast response ionization gauge located on the top of the divertor dome was also two times higher with the divertor puff than with the main puff. Therefore, the following processes might be important in carbon impurity generation with the divertor puff:

(1) the neutral particles on the top of the divertor dome became higher by the gas fueling,

(2) hydrocarbon chemically sputtered from the divertor dome also became larger, and

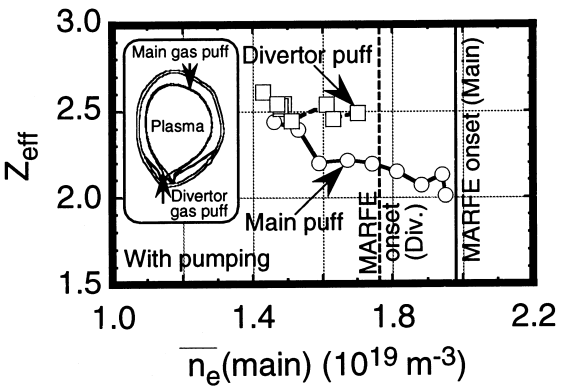

Fig. 5. Z_{eff} values in the main plasma and MARFE onset densities. Circles: main puff with pump. Squares: divertor puff with pump.

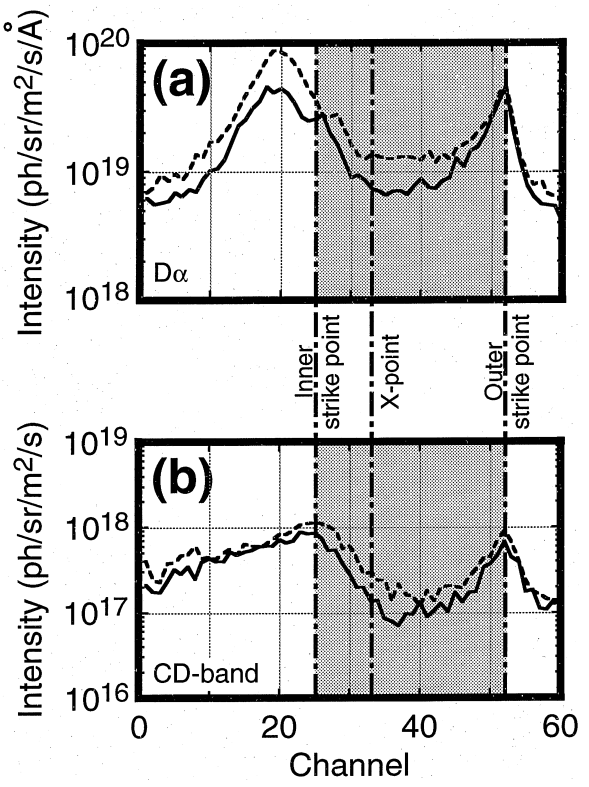

Fig. 6. (a) D_α line and (b) CD-band intensity profiles in the divertor region. The line averaged electron density was 1.6×10^{19} m^{-3} and the pumping system was active. Solid line: main gas puff. Dotted line: divertor gas puff.

(3) carbon impurity originating from hydrocarbon became larger near the x-point. Therefore, the gas puffing with main gas puff was effective in reducing impurity in the main plasma.

6. Summary

The carbon impurity behavior was investigated in the w-shaped pumped divertor of JT-60U. The conclusions are summarized as follows:

(1) The difference of carbon impurity generation in helium and deuterium plasmas indicates that carbon generation by chemical sputtering process is important in deuterium plasmas.

(2) The divertor dome is effective in suppressing the production of hydrocarbon molecules in the private flux region and preventing hydrocarbon molecules from easily reaching the x-point.

(3) The intensity of CD-band calculated with the IMPMC-code agrees well with measurement within a factor of $\sim$2.5.

(4) The Z_{eff} values in the main plasma become lower, and the MARFE onset densities are higher with main gas puff than with divertor gas puff. For reducing carbon impurity in the main plasma, the gas puffing from the top of main plasma is effective.

Acknowledgements

The authors are grateful to the JT-60 team for excellent cooperation. The authors would like to thank Drs. R. Yoshino, A. Funahashi, M. Azumi and H. Kishimoto for continuous support.

References

[1] L. Horton et al., in: 24th EPS Conf. on Contr. Fusion and Plasma Phys., Berchtesgaden, 1997, p. I-65.
[2] S.L. Allen et al., in: 24th EPS Conf. on Contr. Fusion and Plasma Phys., Berchtesgaden, 1997, p. III-1129.
[3] O. Gruber et al., Plasma Phys. Control. Fusion 39 (1997) B19.
[4] N. Hosogane et al., in: 1996 Fusion Energy Conf., Montreal, International Atomic Energy Agency, IAEA-CN-64/GP-11.
[5] H. Kubo et al., J. Nucl. Mater. 196–198 (1992) 71.
[6] A. Sakasai et al., in: IAEA Würzburg 1992, IAEA-CN-56/A-7-12.
[7] K. Shimizu et al., in: IAEA Seville 1994, IAEA-CN-60/D-P-I-2.
[8] S. Higashijima et al., J. Nucl. Mater. 241–243 (1997) 574.
[9] N. Hosogane et al., these Proceedings.
[10] H. Tamai et al., these Proceedings.
[11] J. Roth et al., Nucl. Fusion 1 (Suppl.) (1991) 64.
[12] K. Behringer, J. Nucl. Mater. 176/177 (1990) 606.
[13] K. Itami et al., these Proceedings.